NJC

Accepted Manuscript

This is an *Accepted Manuscript*, which has been through the Royal Society of Chemistry peer review process and has been accepted for publication.

Accepted Manuscripts are published online shortly after acceptance, before technical editing, formatting and proof reading. Using this free service, authors can make their results available to the community, in citable form, before we publish the edited article. We will replace this *Accepted Manuscript* with the edited and formatted *Advance Article* as soon as it is available.

You can find more information about *Accepted Manuscripts* in the Information for Authors.

Please note that technical editing may introduce minor changes to the text and/or graphics, which may alter content. The journal's standard Terms & Conditions and the Ethical guidelines still apply. In no event shall the Royal Society of Chemistry be held responsible for any errors or omissions in this *Accepted Manuscript* or any consequences arising from the use of any information it contains.

ROYAL SOCIETY OF CHEMISTRY

www.rsc.org/njc

New Journal of Chemistry

ARTICLE

A novel water-soluble hydrophobically associating polyacrylamide based on oleic imidazoline and sulfonate for enhanced oil recovery

Shaohua Gou, *[ab] Shan Luo,[b] Tongyi Liu,[b] Peng Zhao,[b] Yang He,[b] Qinglin Pan[b] and Qipeng Guo*[c]

Received 00th January 20xx,
Accepted 00th January 20xx

DOI: 10.1039/x0xx00000x

www.rsc.org/

3-(2-(2-Heptadec-8-enyl-4,5-dihydro-imidazol-1-yl)ethylcarbamoyl)acrylic acid (NIMA), 3-(diallyl-amino)-2-hydroxypropyl sulfonate (NDS), acrylamide (AM) and acrylic acid (AA) were successfully utilized to prepare novel acrylamide-based copolymers (named AM/AA/NIMA and AM/AA/NDS/NIMA) which were functionalized by a combination of imidazoline derivative and/or sulfonate via redox free-radical polymerization. The two copolymers were characterized by infrared (IR) spectroscopy, ^{1}H nuclear magnetic resonance (^{1}H NMR), viscosimetry, pyrene fluorescence probe, thermogravimetry (TG) and differential thermogravimetry (DTG). As expected, the polymers exhibited excellent thickening property, shear stability (viscosity retention rate 5.02% and 7.65% at 1000 s^{-1}) and salt-tolerance (10000 mg/L NaCl: viscosity retention rate up to 17.1% and 10.2%) in comparison with similar concentration partially hydrolyzed polyacrylamide (HPAM). Temperature resistance of AM/AA/NDS/NIMA solution was also remarkably improved that the viscosity retention rate was up to 54.8% under 110 °C. According to the core flooding tests, the oil recovery could be enhanced up to 15.46% by 2000 mg/LAM/AA/NDS/NIMA brine solution at 80 °C.

Introduction

With the development of exploring complicated geologic reservoirs, increasing attention has been paid to maximize to obtain the residual oil, which was retained in the formation after water flooding.[1, 2] Generally, polyacrylamide (PAM) and/or partially hydrolyzed polyacrylamide (HPAM), as a kind of the most prosperous utilized water-soluble polymers in commercial chemical EOR applications,[3-6] impair the viscosity in the presence of high-salinity and deform extremely at high-temperature.[7-9] Furthermore, the thickening power was greatly reduced at elevated shear rate and shear stress, which was associated with the irreversible shear degradation of their linear flexible chains.[10-12]

Recently, hydrophobically associating polymer (HAPAM) that PAM was modified with a small number of various hydrophobic groups has been proposed in oil-field chemical additives by many researchers,[13-16] which can somewhat improve linear flexible chains as a means to preferably resist harsh formation conditions. Numerous efforts have been confirmed that hydrophobic moieties incorporated directly into the backbone of polymers are associated in aqueous phase by intra and intermolecular interaction once above its critical micelle concentration.[17-19] Owing to the reversible dissociation process of physical links, those proved the distinct shear thinning and thixotropy in aqueous solutions under shear rate and shear time. Additionally, high surface and interfacial activities exhibited by most hydrophobic moieties functionalized polymers were found to relate with the presence of hydrophobic groups.[20-22] Commercially, given particular rheological properties, high surface and interfacial activities, the potential of those polymers in EOR applications has been of great concerns of chemical technology as surfactants,[16] flocculation,[15] profile modification,[23, 24] and industrial thickeners,[25] etc.

The solubility of hydrophobically associating polymer in aqueous phase, one of the most considerable requirements in the process of oil exploration, therefore, has been given increasing attention. However, HAPAM implemented in many oil applications, even in laboratory study, has been demonstrated to incompletely disperse in aqueous phase.[26-28] Compared with conventional water-soluble polymers, thereby, HAPAM present poor dissolving capacity with the increase of hydrophobic moieties.[29-32] In parallel with the ongoing discussions on the contribution of hydrophobic long chain to the relative poor solubility of HAPAM, other acrylamide-based polymers functionalized the efficient commoners have been extensively reported in a bid to improve their water solubility in the literature and oilfield chemical applications, for instance, the combination of acrylamide with sulfonamide groups,[33-35] sulfonic acid groups,[36, 37] phosphate groups,[38] zwitterion groups[39, 40] and others exhibited more preferable hydrolysis ability in application process for EOR.

In this article, we had hierarchically synthesized the monomer, namely, 3-(2-(2-heptadec-8-enyl-4,5-dihydro-imidazol-1-yl)ethylcar-

[a] State Key Laboratory of Oil and Gas Reservoir Geology and Exploitation, Southwest Petroleum University, Chengdu, Sichuan 610500, China. E-mail: shaohuagou@swpu.edu.cn.
[b] Oil & Gas Field Applied Chemistry Key Laboratory of Sichuan Province, College of Chemistry and Chemical Engineering, Southwest Petroleum University, Chengdu Sichuan 610500, China.
[c] Polymers Research Group, Institute for Frontier Materials, Deakin University, Locked Bag 20000, Geelong, Victoria 3220, Australia. E-mail: qguo@deakin.edu.au.

† Electronic Supplementary Information (ESI) available: Synthesis routes, and their initial 1H NMR spectrogram analysis of NDS and NIMA; solution preparation and characterization; fluorescence spectra of different concentrations of copolymer solutions; the composition of synthesized brine for dissolving polymer particle samples in the rheological experiments.

bamoyl)acrylic acid (NIMA) with an imidazoline ring structure in conjunction with long aliphatic chain hydrophobic moiety, and the other one, denoted as 3-(diallyl-amino)-2-hydroxypropyl sulfonate (NDS) with sulfonate group. Then, novel water-soluble polymers (named as AM/AA/NIMA and AM/AA/NDS/NIMA, respectively), have been employed to compose of acrylamide (AM), acrylic acid (AA), NIMA and/or NDS via simple free-radical co-polymerization strategy. The infrared spectroscopy (IR), ^{1}H nuclear magnetic resonance (^{1}H NMR), thermogravimetry (TG), differential thermogravimetry (DTG), viscosimetry, and pyrene fluorescence probe were conducted to characterize the morphologies for obtained polymers, respectively. Given the polymers in aqueous solution or brine, whereupon we have further focused on the research of the influence of their unique properties for EOR, such as thickening ability, dissolving capacity, thermal stability, anti-shear degradation, rheological behavior, salt tolerance, resistance factor, residual resistance factor, and EOR value.

Experimental section

Materials

Acrylamide (AM), acrylic acid (AA), sodium bisulfite ($NaHSO_3$), ethanol, sodium hydroxide, ammonium persulfate ($(NH_4)_2S_2O_8$), maleic anhydride (MA), oleic acid, diethylenetriamine, epichlorohydrin, and diallyl amine were both analytical reagent and used directly without further purification treatment. Above the chemicals were purchased from Kelong Chemical Reagent Factory (Chengdu, China), wherein, partially hydrolyzed polyacrylamide (HPAM, 20-30% degree of hydrolysis, M_w=5×10^6). The simulated brine used in this paper was prepared with the inorganic salt on a basis of most formation reservoirs, such as NaCl, KCl, $CaCl_2$, $NaHCO_3$, Na_2SO_4, and $MgCl_2{\cdot}6H_2O$, etc.

Synthesis

Preparation of functionalized comonomers. See supplementary information for the detailed synthesis procedure and synthesis routes of the comonomers NIMA and NDS. Furthermore, the detailed characterization of NIMA and NDS are given in supplementary information.

Synthesis of copolymers AM/AA/NIMA and AM/AA/NDS/NIMA. The indicated amounts of raw materials AM, AA, NIMA and/or NDS were added into a flask with mechanical stirring in deionized water under an inert nitrogen atmosphere. NaOH solution was utilized to regulate the pH to a given value with magnetic stirring for 10-15 min. Copolymerization could be allowed to initiate by the addition of $(NH_4)_2S_2O_8$ and $NaHSO_3$ (molar ratio 1:1) at a stated temperature for a minimum of 6 h. The white granular copolymers, after purified repeatedly through ethanol, were dried at 45-55 ^{o}C under vacuum for approximately 8-12 h. The synthesis routes were shown in Scheme 1.

Pyrene fluorescence probe

The fluorescence intensities were performed with a Shimadzu RF-5301PC pectrofluorophotometer with excitation at 335 nm. A slit width of excitation and emission was fixed at 5 nm and a spectral range was scanning at 350-580 nm with a temperature of 25 ^{o}C. The different concentrations of copolymer solutions were prepared with the saturated aqueous solution of pyrene; the concentration of pyrene was about 2×10^{-6} mol/L.[41] The ratios between the strength of the first peak (I_1) and the third peak (I_3) in fluorescence spectra were calculated.

Water solubility test

The solution conductivity was measured by using a DDS-11A conductivity meter (Shanghai Rex Xinjing Instrument Co., Ltd., China). Polymer particles samples (16-20 meshes) were dispersed and dissolved in deionized water performing at the ambient temperature (about 25 ^{o}C). The water solubility curves were obtained by the dissolution time, which is defined as the time from initially adding the polymer to solution conductivity stabilizing.

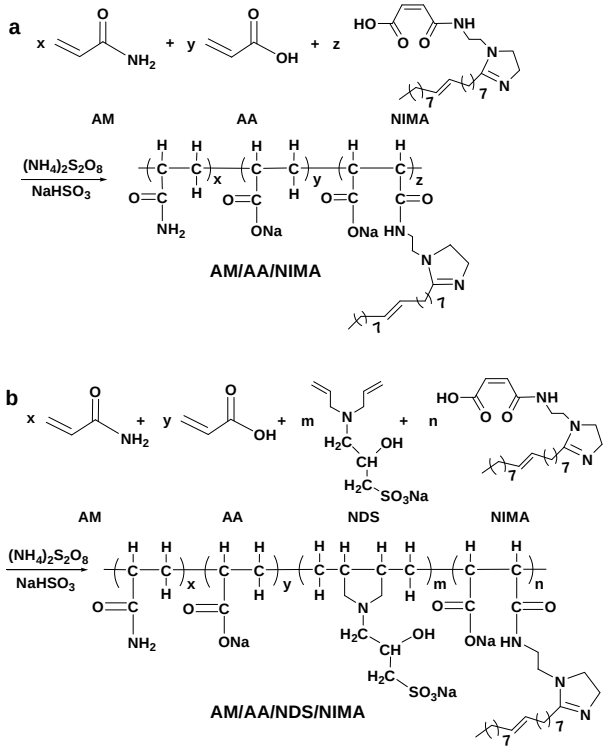

Scheme 1 Synthesis routes of (a) AM/AA/NIMA and (b) AM/AA/NDS/NIMA.

Table 1 Composition of synthetic water flooding

ion	Na^+	K^+	Ca^{2+}	Mg^{2+}	Cl^-	HCO_3^-	SO_4^{2-}	Total
Concentration (mg/L)	2231	70	95	226	4026	28	549	7225

Rheological characterization

The rheological behaviors were managed to measure with an advanced polymer analyzer (Haake RheoStress 6000 rotational rheometer) from Germany. Shear-tolerance measurements were investigated with shear rate ranging from 7.34 to 1000 s^{-1} under a constant temperature of 30 ^{o}C. Shear recovery performance was performed using alternate shear rate between 170 s^{-1} and 510 s^{-1} at

a desired concentration at 30±1 °C. Temperature-resistance tests were conducted by varying temperature from 25 °C to 120 °C under shear rate of 170 s^{-1}. The total salinity of synthetic brine across rheological tests is about 3500 mg/L (see Table S1, ESI†). The polymers solutions were kept stationary to temperature equilibrate for a minimum of 15 min before performing to guarantee that the experiments are mainly accurate. The viscoelastic measurement was carried out with the oscillatory frequency ranging from 0.01 to 10.00 Hz at the steady-state stress under 30 °C.

Core flooding test

A series of one-dimensional sand-packed models were utilized to test the effect of copolymers on enhanced oil recovery by the combination of saturated brine/polymer flooding at 80 °C. The simulated oil (67.4 mPa·s at 80 °C) was prepared as the oil phase in core flooding experiments. The water-flooding across the core plugs was prepared in advance by dissolving different salts in deionized water that the total salinity was about 7200 mg/L (see Table 1). To eliminate capillary side effects, all flooding experiments were performed at an original flow rate of 0.2 mL/min, afterwards, elevated to 0.5 mL/min.

The experiment contains following steps: (1) The simulated crude oil was conducted to infuse the prepared core assembly, wherein the sand was dry for a minimum of 24 hours before performing; (2) For a flow rate of 0.5 mL/min, saline solution was injected to substitute the simulated crude oil until no more oil was produced and the water content was about 95%, wherein the permeability and porosity of the core plugs were estimated by the procedure of replacing the simulated oil; (3) The predissolving copolymer or HPAM solutions were injected to displace salinity water until the pressure difference across the cores was stabilized and no more oil was produced; (4) The subsequent water flooding eventually was injected to replace above polymer solution samples until no more oil was exhausted and the pressure difference for the cores was primarily steady-going.

Results and discussion

The AM/AA/NIMA and AM/AA/NDS/NIMA acrylamide-based polymers were prepared via redox free-radical polymerization of AM, AA, NIMA and/or NDS in the presence of $(NH_4)_2S_2O_8$-$NaHSO_3$. After purification and drying, the viscosities of polymer solutions with desired concentrations were measured under different conditions.

Optimal synthesis conditions of copolymerization

Variation of apparent viscosity of copolymers solutions (1000 mg/L) with different synthesis conditions were identified by a single variable method, which was measured by Brookfield DV-III+Pro Viscometer at room temperature (30 °C), as shown in Fig. 1a-e. It was found that the optimal synthesis conditions for copolymer AM/AA/NIMA were carried out: the initiator concentration is 0.5 wt%; pH value of the solution is 7; the reaction temperature is 40 °C; the ratio of AM and AA on weight is 70:30; loading of NIMA is 1.5 wt‰. Then the result of copolymer AM/AA/NDS/NIMA solution revealed that the maximum apparent viscosity was 379.2 mPa·s at 1000 mg/L, following the matching conditions: the initiator concentration is 0.5 wt%, pH value of the solution is 7, the reaction temperature is 35 °C, the ratio of AM and AA on weight is 65:35, the concentrations of monomer NDS and NIMA are 2.0 wt% and 1.5 wt‰, respectively.

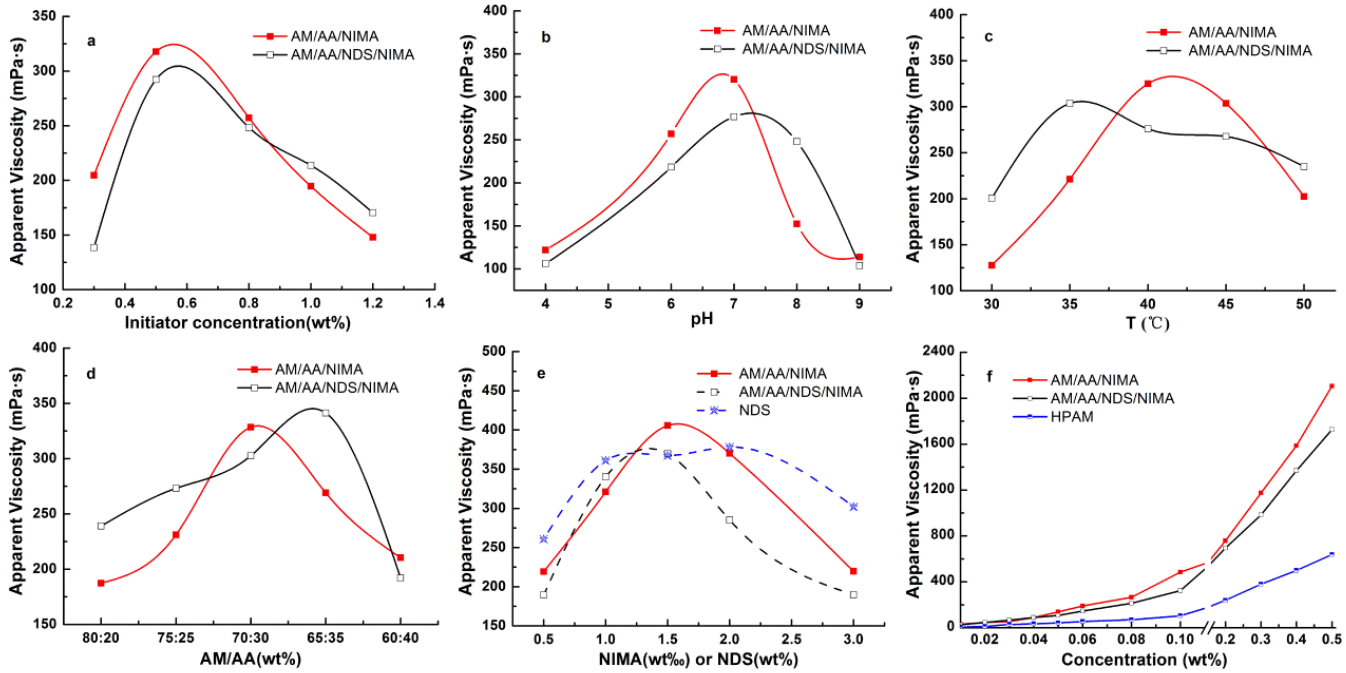

Fig. 1 The influence factors of optimum synthesis condition

The thickening abilities of obtained polymers were confirmed under different magnifications around 30 °C in comparison to HPAM. The apparent viscosity increased by stages along with a strong increase of copolymer concentration ranging of 100-5000

mg/L in aqueous phase. The result demonstrated that the copolymers exert better thickening property than HPAM in Fig. 1(f). And from the curves of viscosity variation of copolymers AM/AA/NIMA and AM/AA/NDS/NIMA, a dramatic increase was detected beyond the concentration of 800 mg/L and 1000 mg/L, respectively. Those revealed that the catastrophe points of obtained polymers are lower than that of HPAM. This phenomenon could be prompted by the strong interchain association and lead the formation of large aggregates as the polymer concentration increased and surpassed its critical level. The high-effect thickening behavior of these associative polymers is contributed significantly to the network structures of polymer chains.

Characteristic analysis

IR analysis. The structures of obtained monomers and copolymers were investigated by an infrared spectrometer, as described in Fig. 2. The copolymers' IR spectra exhibited that the monomers NIMA and/or NDS were successfully introduced into the backbone of PAM molecular chains on account of the characteristic peaks at 3423 cm^{-1}, 1633 cm^{-1}, 1540 cm^{-1}, 1496 cm^{-1}, and 1401 cm^{-1} in AM/AA/NIMA IR spectrum and 3431 cm^{-1}, 1673 cm^{-1}, 1559 cm^{-1}, 1458 cm^{-1}, 1400 cm^{-1}, 1172 cm^{-1}, and 1118 cm^{-1} in IR spectrum of polymer AM/AA/NDS/NIMA. Obviously, the new absorption peaks around 1172 cm^{-1} and 1118 cm^{-1} in AM/AA/NDS/NIMA IR spectrum were attributable to the stretching vibration of $–SO_3^-$ groups, which belong to the bands at 1179 cm^{-1}, 1225 cm^{-1} of $–SO_3^-$ groups in NDS IR spectrum.

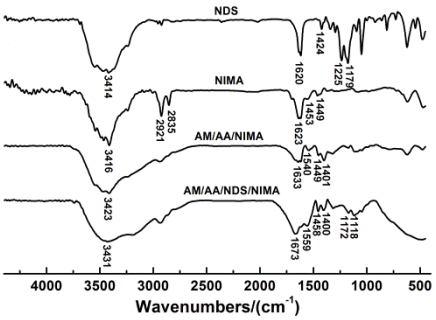

Fig. 2 IR of obtained monomers and copolymers.

^{1}H NMR analysis. From the ^{1}H NMR spectrum of copolymer AM/AA/NIMA in Fig. 3(a), the chemical shift value appeared at 7.66 ppm is assigned to the NH protons of [$CONHCH_2$–]. The chemical shift value owing to the NH protons of [$CONH_2$] is appearing at 6.84 ppm. The chemical shift value at 5.71-5.73 ppm is attributed to –NCH_2– of [$(CH_2)NCH_2CH_2N$=] of the heterocycle of NIMA. The characteristic peak due to –CH_2N= of the imidazoline ring was detected at 3.52-3.71 ppm. The chemical shift value around 5.53-5.56 ppm is the protons of the aliphatic –CH=CH– of [–$CO(CH_2)_7CH$=$CH(CH_2)_7CH_3$], indicating the successful copolymerisation of NIMA monomer. The chemical shift value about 1.06-1.07 ppm was appointed to the –CH_3 proton of the aliphatic chain. The protons of the aliphatic –CH_2– and polymeric chain appeared at 1.52 ppm, and the –CH– protons of polymeric chain were appointed at 1.98-2.34 ppm.

Depicted in Fig. 3(b) was the ^{1}H NMR spectrum of copolymer AM/AA/NDS/NIMA, which revealed the similar morphological characteristics to AM/AA/NIMA. Then the extra peak at 2.82 ppm representing the –CH– protons of [–$CH_2CH(OH)CH_2SO_3Na$], obviously, suggesting that the monomer NDS (see Fig. S1 for the ^{1}H NMR spectrum, ESI†) was successfully polymerized. Owing to the synthesis method by using NaOH solution to adjust pH value across polyreaction, the –OH protons of [–COOH] could not be detected.

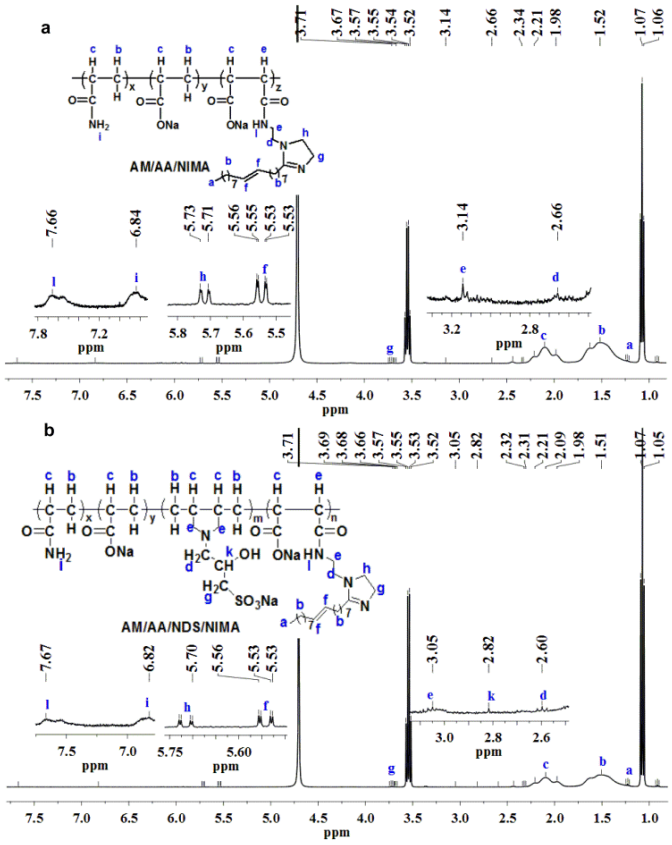

Fig. 3 ^{1}H NMR of copolymers (a) AM/AA/NIMA and (b) AM/AA/NDS/NIMA.

Critical association concentration

The ratios (I_1/I_3) of the intensities of the first and the third peaks in the pyrene probe fluorescence spectrum (called the "polarity scale") were employed to characterize the critical association concentration (CAC) of two copolymers, which is defined as the concentration from intramolecular association beginning to transfer into intermolecular association.[42] The values of I_1/I_3 dependent on concentrations of the copolymers in fluorescence spectra (see Fig. S2, ESI†) were given in Fig. 4. For the curves of I_1/I_3, the I_1/I_3 values decreased abruptly when the concentrations of polymers AM/AA/NIMA and AM/AA/NDS/NIMA surpassed 0.8 g/L and 1.0 g/L, respectively. Those indicated the formation of strongly hydrophobic microdomain due to the intermolecular association, and pyrene molecules transferred into the hydrophobic microdomains, giving rise to the abrupt decrease of I_1/I_3 values owing to the polarity weakening of the microenvironment around pyrene molecule. The results are also obviously discovered in the relationship curves between the viscosity and polymer concentrations in Fig. 1(f).

Water solubility

The displacement system, generally, is prepared with injected water to oil reservoir in many oilfield applications. The solubility of water-soluble hydrophobic associating polymer may decline with hydrophobic moieties increased, however, to restrict application benefit and formation damage. HAPAM, reported in many articles and numerous experimental studies, can increase significantly the viscosity and weaken the solubility of polymer, especially at high overall hydrophobic concentrations. Thereby, solubility of polymers, a crucial factor, should be concerned in the displacement system for EOR.

Presented in Fig. 5 were the conductivity changes in dissolution process that the solubility of the obtained polymers was more prominent than the common hydrophobic associating polymer, and AM/AA/NDS/NIMA required 63 min to dissolve which was shorter than that of AM/AA/NIMA (92 min). Through an attempt with water-soluble polymer functionalized of $-COO^-$ of monomer NIMA and/or sulfonate group of NDS, we found that the presence of those could slow the declining tendency of solubility of the associating polymer. Compared with AM/AA/NIMA, furthermore, copolymer AM/AA/NDS/NIMA exerted preferable water solubility owing to the extra introduction of sulfonate group in the polymer molecular chain.

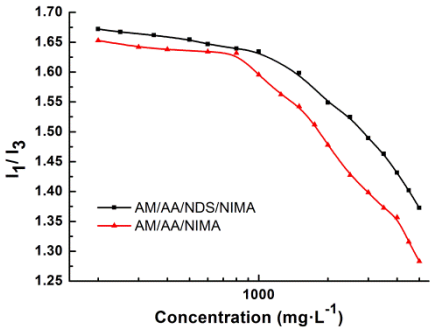

Fig. 4 Effect of different concentrations of copolymers on the I_1/I_3 value.

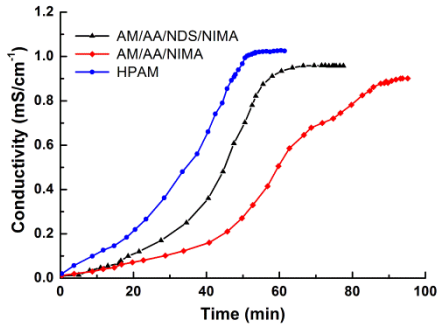

Fig. 5 Curves of conductivity changes in dissolution process of copolymers.

Intrinsic viscosity [η]

Intrinsic viscosity [η] of copolymers AM/AA/NIMA and AM/AA/NDS/NIMA were measured, which can express more of the expanded extent of the molecule chain of copolymer. As expected, it can be readily derived that the intrinsic viscosity of copolymer AM/AA/NIMA and AM/AA/NDS/NIMA were 1149.6 mL/g and 1021.8 mL/g, respectively.

Thermal stability

The mass loss and thermal gravimetric curves of AM/AA/NIMA and AM/AA/NDS/NIMA were depicted in Fig. 6. It was evident that the polymers had three stages for the mass loss as those curves delineated. The first step of AM/AA/NIMA appeared in the range of 25-176 °C with a weight loss of 7.66 wt% owing to the evaporation of intra and intermolecular moisture, which took place in 25-178 °C range with a mass loss of 6.06 wt% for AM/AA/NDS/NIMA. The second one of AM/AA/NIMA occurred in the temperature range of 176-517 °C with a mass loss of 61.74%, which could be associated with the imine reaction of the amide group, and the thermolysis of hydrophobic long chain and imidazoline ring, while that of AM/AA/NDS/NIMA appeared in the 178-484 °C range with a weight loss of 64.31 wt%. The final stage of AM/AA/NIMA appeared above 517 °C with the mass loss corresponding to the carbonization, whereas that of AM/AA/NDS/NIMA occurred beyond 484 °C with mass loss of 10.49 wt%. Obviously, an excess weight loss peak of the DTG curve of AM/AA/NDS/NIMA at the second stage (446 °C) was detected in comparison with AM/AA/NIMA which can be attributed to decomposition of sulfonate group of NDS. Furthermore, it could be observed that the mass loss rate and weight loss of AM/AA/NDS/NIMA were less than that of AM/AA/NIMA comparing the DTG curves of obtained polymers. The results of thermal gravimetric data indicated the copolymers had excellent thermal stability.

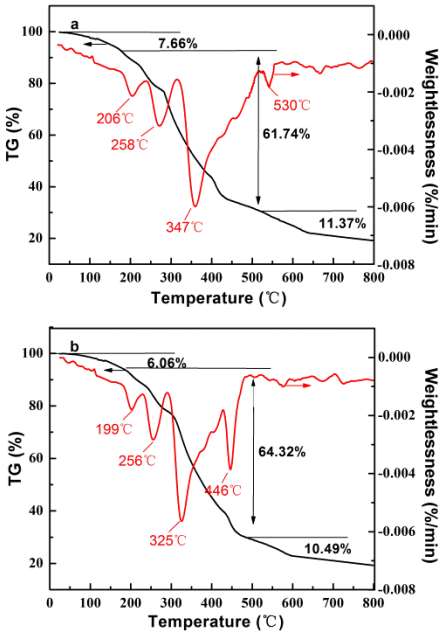

Fig. 6 Mass loss and thermal gravimetric curves of (a) AM/AA/NIMA and (b) AM/AA/NDS/NIMA.

Rheological behavior

Shear resistance. The conventional water-soluble polymer is sensitive to the shear degradation of viscosity at high pressure and high flow rate, which would affect immensely its oilfield application for EOR. Depicted in Fig. 7 were the dependencies of shear rate on

apparent viscosity of obtained polymers and HPAM solutions at a range of certain conditions.

Study of shear stability of the synthesized copolymers in deionized water (2000 mg/L) was delineated in Fig. 7(a). Although a sharp decrease in viscosity accompanied by shear rate rising, the obtained polymers preferably relieved the declining gradually trend of apparent viscosity under high shear stress in comparison to HPAM. The results for copolymer AM/AA/NIMA and AM/AA/NDS/NIMA demonstrated excellent anti-shear degradation that those obtained higher viscosity retention rate about 5.02% and 7.65% at 1000 s^{-1} corresponding to HPAM solution lost most of the viscosity, respectively, while the addition of functional monomer kept an ultralow value.

To further gain insight into the anti-shear behavior, exhibited in Fig. 7(b) were the shear rheological results of the polymers solutions (2000 mg/L) in synthetic brine (see Table S1, ESI†) at 30 ^{o}C. Both the apparent viscosity curves exhibited an unapparent rise initially at low shear rates, but then appeared shear thinning at high shear rate. The phenomena might be attributed to the balance of intra and intermolecular associations which could slightly increase the viscosity at low shear rate, then the disruption and breakage of the network junction followed by further increase in shear rate. [43, 44] It could be concluded that the copolymers exhibited a characteristic of shear-thinning behaviour, which were attributed to the physical reversibility of the association framework.[45, 46]

For polymers AM/AA/NIMA and AM/AA/NDS/NIMA in aqueous phase (2000 mg/L), moreover, an extremely abrupt change of the shear rate after a permanent shear rate lasted for 5 min was depicted in Fig. 7(c). It was discovered the apparent viscosity of the previous polymer solutions have been practically undergone a flipping back and forth with the shear rate ranged from 170 s^{-1} to 510 s^{-1}, then back again to 170 s^{-1}. Although a slight decline in viscosity occurred at higher shear rate on account of the part disruption of networks structure, the obtained polymers exhibited satisfying shear stability. As the shear rate and shear stress increasing, however, the three-dimensional network structures of polymer chains issued from intermolecular association effect are more likely to strive against and give rise to, consequently, high-shear resistance.

Temperature tolerance. For polymer concentration of 2000 mg/L in aqueous phase, an almost temperature dependent on viscosity was observed at a constant shear rate, as depicted in Fig. 8(a). At low temperature, an unconspicuous decrease in viscosity was initially observed, which can be attributed to intermolecular assemblies of polymer modified hydrophobic groups. With the temperature rising, the progressive rupture of intermolecular aggregation of the network structure would affect the molecular weight of polymer, and hence lead to a decrease in solution viscosity. AM/AA/NIMA and AM/AA/NDS/NIMA solutions displayed high temperature tolerance at 110 ^{o}C compared with that under 25 ^{o}C, and had the viscosity retention rate of 40.5% and 54.8%, respectively. Those could be explained by the hydrophobic effect of NIMA and the stiff microstructure of imidazoline ring, and/or the ability of NDS to form strong hydrogen-bonding,[47] which could sustain higher viscosity retention rate under high-temperature.[48]

Fig. 8(b) was exhibited to further gain insight into the temperature resistance of the obtained polymers solutions (2000 mg/L) in synthetic brine (see Table S1, ESI†) at 170 s^{-1}. It could be observed that both apparent viscosity of the synthesized polymers solutions were almost stable initially, but then decreased gradually with the temperature rising. However, a distinct difference, compared the two curves, was easily observed that AM/AA/NDS/NIMA presented better viscosity retention rate (about 23.7%) than that of AM/AA/NIMA (about 16.9%) under the temperature of 90 ^{o}C. The phenomena can be explained that incorporating electronic charges and hydrophobic group into water-soluble polymer can control the interaction of the intra and intermolecular between the polymer chains and increase their stability in brine, which makes the corresponding solutions less sensitive to the external temperature on apparent viscosity.[49]

The influence of temperature for the copolymer solutions (2000 mg/L) in deionized water was investigated with range of 25-120 ^{o}C at three kinds of shear rate (170 s^{-1}, 270 s^{-1} and 370 s^{-1}, respectively), as shown in Fig. 8(c). As expected, it can be observed that the apparent viscosity gradually decreased with the increase of shear rate and temperature from those curves for the polymer solutions. Besides, the influence of temperature was more prominent at higher shear rate where the disruption of the intermolecular association effect is more pronounced compared to that of low shear rate. The phenomena can be explained by the weakening of hydrophobic effect at high temperature, which can lead to the increased mobility of the polymer chain and the loss of interchain interaction as the temperature increases.[50]

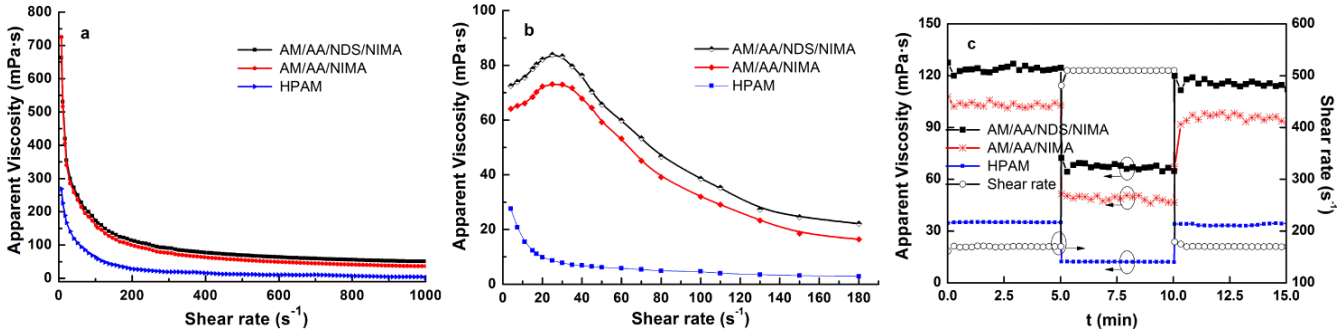

Fig. 7 Effect of shear rate on apparent viscosity in (a) aqueous phase and (b) synthetic brine; (c) shear recovery at different shear rates.

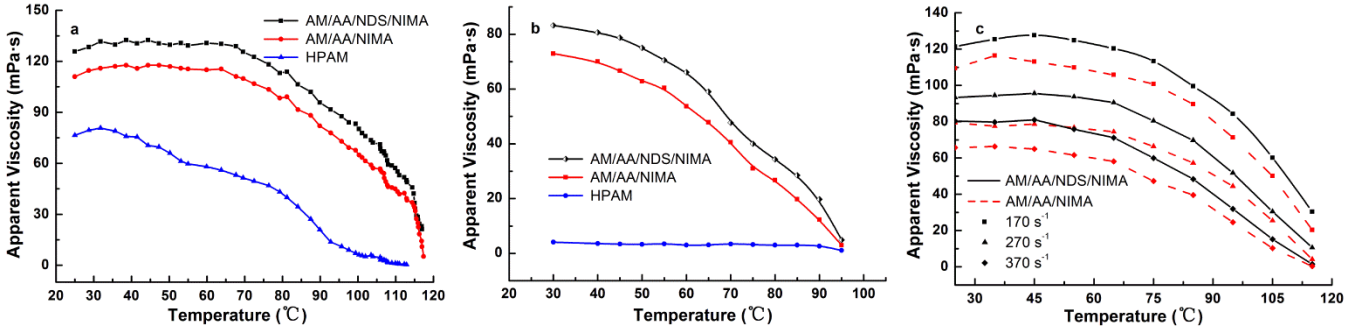

Fig. 8 Effect of temperature on apparent viscosity in (a) aqueous phase and (b) synthetic brine; (c) temperature tolerance at different shear rates.

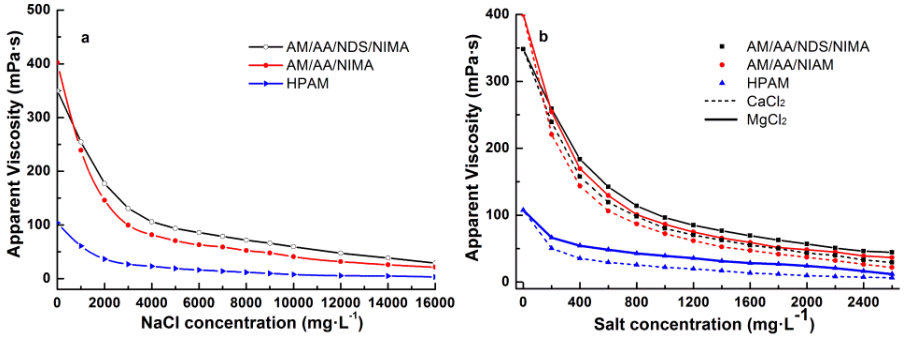

Fig. 9 Variation of apparent viscosities of copolymers solutions with different (a) NaCl and (b) $CaCl_2$/$MgCl_2$ concentrations.

Salt resistance

Fig. 9(a) was exhibited the ability against Na^+ of obtained copolymers with 1000 mg/L and the tests to resist Ca^{2+} or Mg^{2+} were shown in Fig. 9(b). The viscosity residual rate for copolymers AM/AA/NIMA and AM/AA/NDS/NIMA solutions could be up to 17.1% and 10.2% in 10000 mg/L of NaCl solution, and then up to 12.1% and 9.3% in 2000 mg/L $CaCl_2$, 16.3% and 12.4% in 2000 mg/L $MgCl_2$, respectively. Compared with HPAM, the copolymers represent remarkable salt tolerance owing to the interaction of the long carbon chain of NIMA and the enhanced internal rotation resistance relating to the sulfonate groups.[51] Additionally, those results also demonstrated that the copolymers have preferable salt-resistance to monovalent salt than divalent salt.

Viscoelasticity

The viscoelastic properties as a function of the oscillation frequency for copolymer AM/AA/NIMA and AM/AA/NDS/NIMA solutions (2000 mg/L) were researched via Haake RheoStress 6000 rotational rheometer. The variation of dynamic system was curved by the slope of the storage modulus G', the loss modulus G'' and the crossing point G_c, which were dependent on frequency (see Fig.10). As indicated in Fig. 10, thereby, viscous behavior was observed when G' is less than G'' in the course of the low-frequency region. Then G' and G'' increased gradually accompanying with the oscillation frequency rising, and elastic behavior predominated once the G' value surpassed the G'' value, namely, above the frequency at which the curves cross each other G_c. This is great potential to enhance oil recovery in EOR applications attributed to the typical viscoelastic behaviour of HAPAM solutions.[52]

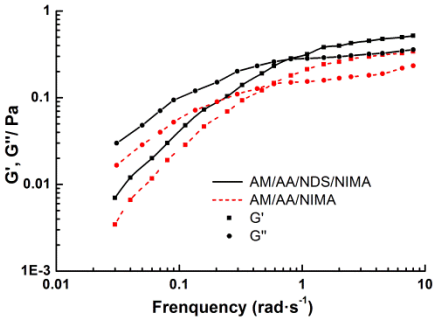

Fig. 10 Variation of viscoelastic properties with the oscillation frequency for copolymer solutions.

Core flooding analysis

Profile control ability. Depicted in Fig. 11 was the flooding pressure profile as function of injected volume (PV) for 2000 mg/L copolymer solutions and post water flooding. From the curves, it can be observed that the climbing flooding pressure presented three types, thereof the pressure increased along with the increased flooding pressure differential during the injection of polymer solutions. The flooding pressure was raised gradually at the onset of polymer flooding after 5 PV of water flooding. It can be recognized that the pressure was further upgraded, whereas declined rapidly to a platform value in the wake of the injection of post water flooding. Polymer particle try to enter larger porous channel associated with its physical selection, afterwards, further migrate and start to accumulate which give rise to the injection pressure elevated and to facilitate the post water flooding diverting. Moreover, it would be formed resistance to restrain its motion, while more amount of polymer solutions migrated into

porous medium as the flooding pressure and injection pressure differential constantly elevated. Obviously, the profile control abilities of obtained polymers were prominent than HPAM that elucidated by the curves of flooding pressure as a function of injected volume.

Illustrated in Table 2 were the characteristic parameters for polymer solutions samples by core flooding experiments, such as initial flooding pressure, breakthrough pressure, stable pressure, resistance factor (*RF*), and residual resistance factor (*RRF*). And, apparently, it can be observed that the two copolymers containing hydrophobic side chain exhibited superior profile control capability, whereby AM/AA/NDS/NIMA had preferable potential in the profile controlled application for enhanced oil recovery, which was associated with its higher stable flooding pressure region in comparison to AM/AA/NIMA and HPAM solutions.

Enhanced oil recovery. The results of AM/AA/NDS/NIMA solutions in core flooding tests were investigated under the simulated salinity oil reservoir environment, as shown in Fig. 12. Compared with HPAM (EOR of 1000 mg/L solution = 3.29 %), the values of obtained polymer solutions for EOR were up to 7.04% (1000 mg/L) and 11.52 % (1500 mg/L), respectively. It was conspicuous that the value about 15.46% more oil recovery could be obtained by AM/AA/NDS/NIMA solution (2000 mg/L) after water flooding. Furthermore, it was obviously discovered that the EOR effect of AM/AA/NDS/NIMA was much better than that of AM/AA/NIMA under the same concentration in water phase.

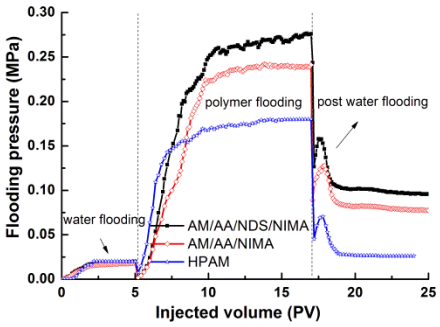

Fig. 11 Effect of injected volume to flooding pressure.

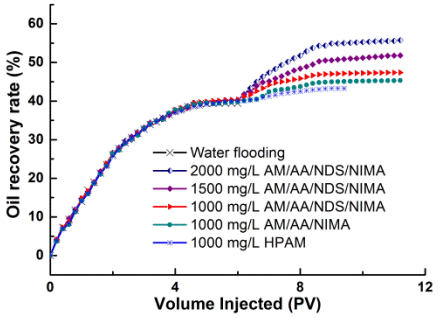

Fig. 12 Results of the core-flooding experiments.

Table 2 Characteristic parameters in core-flooding experiments

Core samples	Core parameter				Polymer solutions samples	Pressure parameter / MPa			Resistance factor	Residual resistance factor
	Diameter /cm	Length /cm	Permeability /$10^{-2}\mu m^2$	Porosity /%		Initial pressure	Breakthrough pressure	Stable pressure		
1	2.501	50.04	7.840	23.60	AM/AA/NIMA	0.0185	0.2411	0.0773	13.03	4.18
2	2.498	50.02	7.838	23.59	AM/AA/NDS/NIMA	0.0199	0.2723	0.0956	13.68	4.80
3	2.503	49.98	7.841	23.62	HPAM	0.0201	0.0705	0.0263	3.51	1.31

Conclusions

A novel imidazoline derivative and/or sulfonate have been successfully synthesized and introduced into polyacrylamide chain via simple free-radical co-polymerization. The critical association concentrations of synthetic polymers due to the dynamics transformation between intra and intermolecular junctions were in the vicinity of 0.8 g/L and 1.0 g/L, respectively, suggesting the hydrophobic microdomains aggregation. High thermostability of the terpolymer and quadripolymer were exhibited that the viscosity residual rates were up to 40.5% and 54.8% at 110 ^{o}C in comparison to that of 25 ^{o}C, respectively. The polymers also exhibited excellent water solubility, shear thinning (residual viscosity of 50.7 mPa·s and 36.4 mPa·s at 1000 s^{-1}), shear recovery and salt resistance. The results of core flooding tests signified that the polymer solutions had stronger mobility control abilities and improved effectively oil recovery. Above outstanding features inferred that obtained polymers had a potential technological interest in high-temperature and high salinity oil recovery or other commercial applications.

Acknowledgements

The work was financially supported by Foundation of Youth Science and Technology Innovation Team of Sichuan Province (2015TD0007), Sichuan Provincial Science and Technology Department (13TD0025), and the Scientific Research Starting Project of Southwest Petroleum University (2014PYZ008). The authors express their sincere thanks for the financial supporters.

Notes and references

1 Q. Chen, Y. Wang, Z. Lu and Y. Feng, *Polym. Bull.*, 2013, **70**, 391-401.
2 C. Zou, T. Gu, P. Xiao, T. Ge, M. Wang and K. Wang, *Ind. Eng. Chem. Res.*, 2014, **53**, 7570-7578.
3 C. Zhong, P. Luo, Z. Ye and H. Chen, *Polym. Bull.*, 2009, **62**, 79-89.
4 C. Chelaru, I. Diaconu and I. Simionescu, *Polym. Bull.*, 1998, **40**, 757-764.
5 J. Hou, *J. Petrol. Sci. Eng.*, 2007, **59**, 321-332.
6 W. Kulicke, R. Kniewske and J. Klein, *Prog. Polym. Sci.*, 1982, **8**,

373-468.
7 W. M. Leung, D. E. Axelson and J. D. Van Dyke, *J. Polym. Sci. A-Polym. Chem.*, 1987, **25**, 1825-1846.
8 A. Sabhapondit, A. Borthakur and I. Haque, *J. Appl. Polym. Sci.*, 2003, **87**, 1869-1878.
9 H. Kheradmand, J. François and V. Plazanet, *Polymer*, 1988, **29**, 860-870.
10 R. S. Seright, J. M. Seheult and T. Talashek, *Spe Reserv. Eval. Eng.*, 2009, **12**, 783-792.
11 S. E. Morgan and C. L. McCormick, *Prog. Polym. Sci.*, 1990, **15**, 103-145.
12 Y. Guo, J. Liu, X. Zhang, R. Feng, H. Li, J. Zhang, X. Lv and P. Luo, *Energ. Fuel.*, 2012, **26**, 2116-2123.
13 A. C. Lara-Ceniceros, C. Rivera-Vallejo and E. J. Jiménez-Regalado, *Polym. Bull.*, 2007, **58**, 425-433.
14 T. Wan, C. Zou, L. Chen, Z. Zhou, M. Xu, W. Cheng and R. Li, *J. Solu. Chem.*, 2014, **43**, 1947-1962.
15 G. O. Yahaya, A. A. Ahdab, S. A. Ali, B. F. Abu-Sharkh and E. Z. Hamad, *Polymer*, 2001, **42**, 3363-3372.
16 K. C. Taylor and H. A. Nasr-El-Din, *J. Petrol. Sci. Eng.*, 1998, **19**, 265-280.
17 S. Biggs, A. Hill, J. Selb and F. Candau, *J. Phys. Chem.*, 1992, **96**, 1505-1511.
18 I. Iliopoulos, T. K. Wang and R. Audebert, *Langmuir*, 1991, **7**, 617-619.
19 Y. Kakizawa, H. Sakai, K. Nishiyama, M. Abe, H. Shoji, Y. Kondo and N. Yoshino, *Langmuir*, 1996, **12**, 921-924.
20 B. F. Abu Sharkh, G. O. Yahaya, S. A. Ali and I. W. Kazi, *J. Appl. Polym. Sci.*, 2001, **82**, 467-476.
21 H. A. Nasr-El-Din, B. F. Hawkins and K. A. Green, *SPE*, 1991, **21028**, 20-22.
22 N. Hameed, J. Liu and Q. Guo, *Macromolecules*, 2008, **41**, 7596-7605.
23 Y. Wang, Y. Dai, L. Zhang, L. Luo, Y. Chu, S. Zhao, M. Li, E. Wang and J. Yu, *Macromolecules*, 2004, **37**, 2930-2937
24 S. Vossoughi, *J. Petrol. Sci. Eng.*, 2000, **26**, 199-209.
25 Y. Feng, L. Billon, B. Grassl, G. Bastiat, O. Borisov and J. François, *Polymer*, 2005, **46**, 9283-9295.
26 Z. Guozhong, X. Minghui, L. Min, W. U. Huaxiao, L. Xiangli and Y. U. Peiqing, *Chinese J. Chem. Eng.*, 2010, **18**, 170-174.
27 S. W. Shalaby, C. L. McCormick and G. B. Butler, *Am. Chem. Soc.*, 1991.
28 P. M. Budd, *Special Publications of the Royal Society of Chemistry*, 1996, **186**, 1-9.
29 K. C. Taylor and H. A. Nasr-El-Din, *J. Petrol. Sci. Eng.*, 1998, **19**, 265-280.
30 R. J. English, J. H. Laurer, R. J. Spontak and S. A. Khan, *Ind. Eng. Chem. Res.*, 2002, **41**, 6425-6435.
31 P. Kujawa, J. M. Rosiak, J. Selb and F. Candau, *Macromol. Chem. Phys.*, 2001, **202**, 1384-1397.
32 K. Inomata, R. Doi, E. Yamada, H. Sugimoto and E. Nakanishi, *Colloid. Polym. Sci.*, 2007, **285**, 1129-1137.
33 K. D. Branham, G. S. Shafer, C. E. Hoyle and C. L. McCormick, *Macromolecules*, 1995, **28**, 6175-6182.
34 X. Xie and T. E. Hogen-Esch, *Macromolecules*, 1996, **29**, 1734-1745.
35 S. Gou, T. Yin, Z. Ye, W. Jiang, C. Yang, Y. Ma, M. Feng and Q. Xia, *J Appl. Polym. Sci.*, 2014, **131**, 40727.
36 A. Sabhapondit, A. Borthakur and I. Haque, *Energ. Fuel.*, 2003, **17**, 683-688.
37 A. Sabhapondit, A. Borthakur and I. Haque, *J. Appl. Polym. Sci.*, 2003, **87**, 1869-1878.
38 D. Wang, C. G. Williams, Q. Li, B. Sharma and J. H. Elisseeff, *Biomaterials*, 2003, **24**, 3969-3980.
39 V. A. Vasantha, S. Jana, A. Parthiban and J. G. Vancso, *Chem. Commun.*, 2014, **50**, 46-48.
40 E. E. Kathmann, L. A. White and C. L. McCormick, *Macromolecules*, 1997, **30**, 5297-5304.
41 J. Huang, X. Li and Q. Guo, *Eur. Polym. J.*, 1997, **33**, 659-665.
42 B. Gao, H. Guo, J. Wang and Y. Zhang, *Macromolecules*, 2008, **41**, 2890-2897.
43 Y. Chang and C. L. McCormick, *Macromolecules*, 1993, **26**, 6121-6126.
44 E. Volpert, J. Selb and F. Candau, *Polymer*, 1998, **39**, 1025-1033.
45 I. Nahringbauer, *J. Colloid Interf. Sci.*, 1995, **176**, 318-328.
46 I. Nahringbauer, *Langmuir*, 1997, **13**, 2242-2249.
47 S. Zheng, Q. Guo, and M. Mi, *J. Polym. Sci. Part B: Polym. Phys.,* 1998, ***36***, 2291-2300.
48 M. Rashidi, A. M. Blokhus and A. Skauge, *J. Appl. Polym. Sci.*, 2011, **119**, 3623-3629.
49 E. E. Tucker, E. H. Lane and S. D. Christian, *J. Solu. Chem.*, 1981, **10**, 1-20.
50 B. F. Abu Sharkh, G. O. Yahaya, S. A. Ali, E. Z. Hamad and I. M. Abu Reesh, *J. Appl. Polym. Sci.*, 2003, **89**, 2290-2300.
51 M. Rashidi, A. M. Blokhus and A. Skauge, *J. Appl. Polym. Sci.*, 2010, **117**, 1551-1557.
52 Z. Ye, M. Feng, S. Gou, M. Liu, Z. Huang and T. Liu, *J. Appl. Polym. Sci.*, 2013, **130**, 2901-2911.